

Month 2019 Et₃N-Prompted Efficient Synthesis of Anthracenyl Pyrazolines and Their Cytotoxicity Evaluation against Cancer Cell Lines

Thechano Merry,^a Prabhakar Maddela,^{a*} Kiran Devaraya,^b Anand K. Kondapi,^b and Chullikkattil P. Pradeep^c

^aDepartment of Chemistry, Nagaland University, Lumami, Nagaland 798627, India

^bDepartment of Biotechnology & Bioinformatics, School of Life Sciences, University of Hyderabad, Hyderabad 500046, India

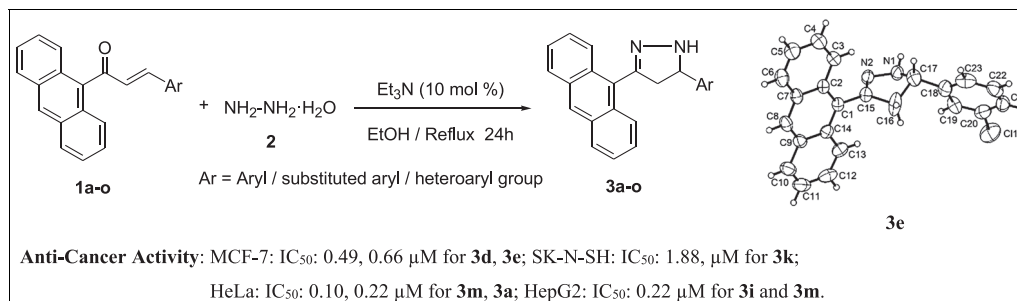
^cSchool of Basic Sciences, Indian Institute of Technology Mandi, Mandi, Himachal Pradesh 175001, India

*E-mail: prab.chem@gmail.com

Received March 25, 2019

DOI 10.1002/jhet.3636

Published online 00 Month 2019 in Wiley Online Library (wileyonlinelibrary.com).



A series of anthracenyl pyrazoline derivatives (**3a–o**) were synthesized with an aim to evaluate their *in vitro* anticancer activities. Anthracenyl pyrazoline compounds were prepared by the reaction between various anthracenyl chalcones (**1a–o**) and hydrazine hydrate (**2**). The reactions were carried out under reflux in the presence of triethylamine and ethanol for 24 h, and the obtained yields were from good to excellent (90–97%). The structure of each compound is well characterized by IR, ¹H-NMR, ¹³C-NMR, elemental analyses, and mass spectroscopic techniques, and the molecular structures of compounds **3d** and **3e** were solved by single-crystal X-ray crystallographic methods. The newly synthesized compounds (**3a–o**) were evaluated for their *in vitro* cytotoxic studies against four human cancer cell lines MCF-7 (breast cancer cell lines), SK-N-SH (neuroblastoma cancer cell lines), HeLa (cervical cancer cell lines), and HepG2 (liver cancer cell lines), and the screening results show strong cytotoxic effects for most of the synthesized compounds against the three cell lines except SK-N-SH cells. Notably, compounds **3a**, **3j**, **3l**, **3m**, **3n**, and **3o** showed a highly potential activity against HeLa cells (IC₅₀: 0.22, 0.3, 0.3, 0.10, 0.25, and 0.25 μM), while compounds **3i**, **3k**, **3l**, and **3m** showed a significant cytotoxic activity in HepG2 cells (IC₅₀: 0.22, 0.44, 0.40, and 0.22 μM), whereas compounds **3a**, **3b**, **3d**, and **3e** exhibit a promising cytotoxicity against MCF-7 cells (IC₅₀: 0.73, 0.495, 0.493, and 0.66 μM).

J. Heterocyclic Chem., **00**, 00 (2019).

INTRODUCTION

Cancer, certainly cancer has become one of the most major health problems in the world, and it affects people at all ages. The World Health Organization reported that 70% or more of all cancer deaths happen in low-income as well as in middle-income nations.[1] All-inclusive, the most noticeable types of cancer are lung, bronchus, prostate, breast, colon, and rectum,[2,3] and it is because of the common environmental factors like use of tobacco, other dietary habits, obesity, infections, radiation, stress, lack of physical activity, and environmental pollutants leading to cancer deaths.[4] Despite extensive research and advances in cancer therapy, cancer is reported to be the second leading cause of death in the world next to cardiovascular disorders.[5–8] Therefore, search for the new potent anticancer agents remains a challenge and need of the hour to fight against cancer disease.

Various naturally occurring and synthetic compounds have been reported for their anticancer activity, and most of them consist of pyrazole unit as the core structure.[9] In particular, pyrazoles are important in medicinal chemistry and were exclusively reported to exhibit wide range of biological properties.[10–12] In the past few decades, extensive research has been carried out on the pyrazole nucleus and its anticancer activity.[13] Therefore, pyrazole is a versatile lead compound to design potent bioactive molecules for drug discovery and development, especially in cancer therapy. Pyrazolines can be considered as intermediate compound for synthesis of various heterocyclic compounds of high biological activity. The well-established methods for the synthesis of substituted pyrazoles are based either on the condensations of substituted hydrazines with dicarbonyl or on intermolecular [3+2] cycloaddition reaction of alkynes 1 to 3-dipoles.[14,15] The addition of a pyrazoline ring between the two aryl rings of chalcone

gives more scope for the synthesis of the new heterocyclic compounds from diverse chalcones.

In view of the aforementioned findings in cancer research and in continuation with our ongoing research in designing and synthesizing natural products-based new scaffolds synthesis and their biological activity, in this article, we report the synthesis of a series of anthracenyl pyrazoline derivatives (**3a–o**) and their anticancer activity evaluation against the MCF-7, SK-N-SH, HeLa, and HepG2 cancer cell lines.

RESULTS AND DISCUSSION

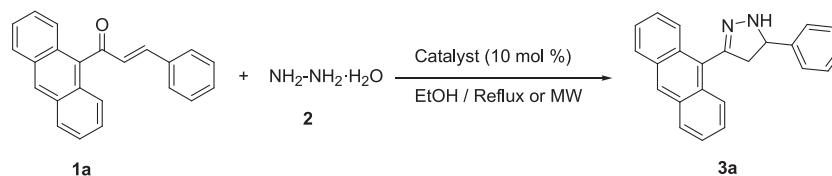
Chemistry. The synthesis of anthracenyl pyrazoline derivatives (**3a–o**) was carried out from the reaction of anthracenyl chalcones (**1a–o**) [16] with hydrazine hydrate (**2**) in the presence of triethylamine (Et_3N) in ethanol solution at refluxing temperature for 24 h. Initially, attempts have made to synthesize the 3-anthracen-9-yl-5-phenyl-4,5-dihydro-1*H*-pyrazole (**3a**) starting from 1:10 ratio of 1-anthracen-9-yl-3-phenyl-propenone (**1a**) with hydrazine hydrate (**2**) in the presence of different acid catalysts (AcOH, HCl, H_2SO_4 , TsOH, and FeCl_3) in ethanol solution under reflux conditions for 24 h, and we observed that the progress of the reactions was very slow and obtained poor yields (Table 1, entries 1–5). Further, we carry out the reaction under microwave reaction conditions at 200°C for 30 min by using different acid catalysts (AcOH, HCl, H_2SO_4 , TsOH, and FeCl_3); here in this reaction also, the percentage of the

yields are not improved much under this methods (Table 1, entries 1–5).

The aforementioned catalysts and conditions were not attained up to satisfactory yields of the product **3a** monitored by thin-layer chromatography (TLC) on time intervals. Then we proceed to carry out the reactions in the presence of base catalysts, such as Et_3N (Table 1, entry 6), piperidine (Table 1, entry 7), and pyridine (Table 1, entry 8) under the refluxing conditions in ethanol for 24 h and microwave conditions, and we found that the better yields (96%) were achieved only in the presence of Et_3N under the refluxing conditions in ethanol for 24 h (Table 1, entry 6). Thus, in order to standardize the reaction, we examined the mole ratio of the reactants (1:1, 1:2, 1:5, and 1:10) for better conversion of the reactant **1a** to the product **3a** in the presence of Et_3N (10 mol %), and we found that the better yields (96%) of the product **3a** were obtained at 1:10 mole ratio of reactants anthracenyl chalcone (**1a**) and hydrazine hydrate (**2**) in ethanol at reflux temperature for 24 h (Table 1, entry 6). To test the generality and scope of this method, we then examined the reactions with a series of anthracenyl chalcones (**1a–o**) and hydrazine hydrate (**2**) under the aforementioned standardized reaction conditions for the synthesis of anthracenyl pyrazoline derivatives (**3a–o**) as revealed in Scheme 1 and Figure 1. All the reactions showed to be a good and quite efficient synthetic etiquette for aryl as well as hetero-aryl group and irrespective of the presence of electron-donating and electron-withdrawing functional groups in phenyl ring system.

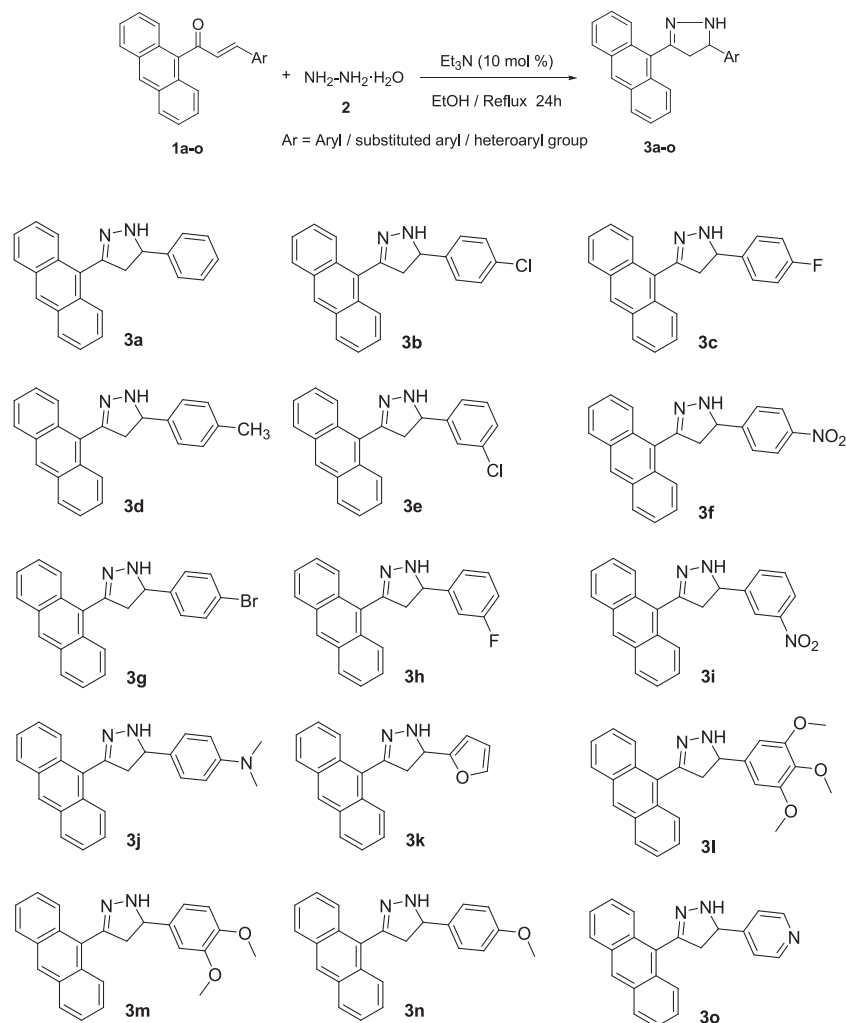
Table 1

Optimization of the reaction conditions and catalysts for the synthesis of anthracenyl pyrazoline (**3a**).^a



Entry	Catalyst	Reaction methods, yields (%)	
		Reflux (24 h)	Microwave (200°C, 30 min)
1	AcOH	30	10
2	TsOH	40	25
3	HCl	35	20
4	H_2SO_4	10	3
5	FeCl_3	10	3
6	Et_3N	96	60
7	Piperidine	40	15
8	Pyridine	25	5

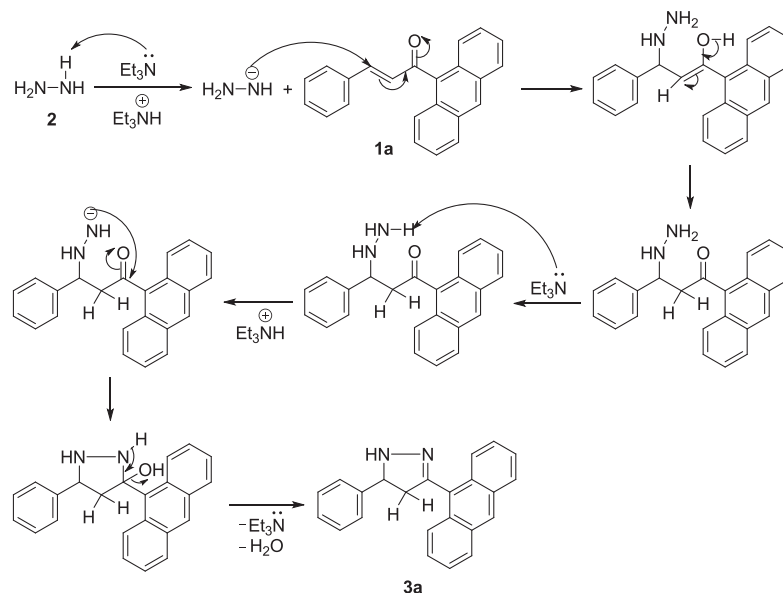
^aReaction conditions: anthracenyl chalcone (**1a**) (1 mmol), hydrazine hydrate (**2**) (10 mmol), and catalyst (10 mol %) in 5 mL ethanol solution.

Scheme 1. Synthesis of anthracenyl pyrazoline derivatives (**3a–o**).Figure 1. Structures of the anthracenyl pyrazoline derivatives (**3a–o**).

The structures of the newly synthesized anthracenyl pyrazoline derivatives (**3a–o**) were elucidated by IR, ¹H-NMR, ¹³C-NMR, and mass spectroscopy. The Fourier transform infrared spectra of the compounds endorse that the disappearance of two absorption bands of the CH=CH and C=O groups of anthracenyl chalcones and appearance of a new absorption bands of NH and C=N groups at 3343 and 1591 cm⁻¹ as well as the aliphatic C–H stretching vibrations appear at 2985–2930 cm⁻¹, respectively. In the ¹H-NMR spectra of the anthracenyl pyrazolines, the CH₂ protons of pyrazoline ring resonated as a pair of doublet of doublets at δ 3.16–3.07 ppm, 3.60–3.51 ppm, and the CH proton of the compounds appears as a triplet at δ 5.35–5.10 ppm because of the protons of the methylene (CH₂) group. In the ¹³C-NMR spectra of the compounds, the characteristic chemical shift values of the pyrazoline ring carbons appear at

47.75–43.71 (C, CH₂ pyrazoline), 64.73–57.48 (C, CH pyrazoline), and 151.80–151.34 (C, C=N pyrazoline) that agree the pyrazoline character deduced from the ¹H-NMR spectra. The proposed reaction mechanism for the synthesis of anthracenyl pyrazolines is shown in Scheme 2.

X-ray crystallography. The molecular structures of the anthracenyl pyrazoline compounds **3d** and **3e** were unambiguously deduced by single-crystal X-ray diffraction analyses. The crystal structure refinement data of **3d** and **3e** are listed in Table 2. The complete listing of the bond distances and bond angles is presented in the supporting information. ORTEP drawings of the crystal structures of **3d** and **3e** with atomic numbering scheme are shown in Figure 2. Compound **3d** crystallized in orthorhombic Pbc_a space group. The asymmetric unit of **3d** consists of two independent molecules as shown in Figure 2, which show almost identical structural features

Scheme 2. Proposed reaction mechanism for the synthesis of anthracenyl pyrazolines (**3a–o**).**Table 2**The single-crystal X-ray molecular structures refinement data of anthracenyl pyrazolines **3d** and **3e**.

Parameters	3d	3e
Empirical formula	C ₂₄ H ₂₀ N ₂	C ₂₃ H ₁₇ ClN ₂
Formula weight	336.42	356.84
Temperature (K)	293(2)	293(2)
Crystal system	Orthorhombic	Orthorhombic
Space group	Pbca	Pccn
<i>a</i> (Å)	18.3899(6)	23.7241(9)
<i>b</i> (Å)	16.2601(5)	15.2117(7)
<i>c</i> (Å)	25.0633(6)	10.1917(4)
α (°)	90.00	90.00
β (°)	90.00	90.00
γ (°)	90.00	90.00
Volume (Å ³)	7494.5(4)	3678.0(3)
<i>Z</i>	16	8
ρ_{calc} (g/cm ³)	1.193	1.289
μ (mm ⁻¹)	0.537	1.885
<i>F</i> (000)	2848.0	1488.0
Crystal size (mm ³)	0.236 × 0.105 × 0.088	0.656 × 0.088 × 0.069
Radiation	CuK α (λ = 1.54184)	CuK α (λ = 1.54184)
2 θ range for data collection (°)	8.54 to 133.62	6.9 to 133.72
Index ranges	-21 ≤ <i>h</i> ≤ 13, -16 ≤ <i>k</i> ≤ 19, -22 ≤ <i>l</i> ≤ 29	-22 ≤ <i>h</i> ≤ 28, -14 ≤ <i>k</i> ≤ 18, -12 ≤ <i>l</i> ≤ 11
Reflections collected	15250	6762
Independent reflections	6476 [<i>R</i> _{int} = 0.0427, <i>R</i> _{sigma} = 0.0462]	3077 [<i>R</i> _{int} = 0.0262, <i>R</i> _{sigma} = 0.0313]
Data/restraints/parameters	6476/0/471	3077/0/235
Goodness of fit on <i>F</i> ²	1.023	1.281
Final <i>R</i> indexes [<i>I</i> ≥ 2 σ (<i>I</i>)]	<i>R</i> ₁ = 0.0646, <i>wR</i> ₂ = 0.1773	<i>R</i> ₁ = 0.1089, <i>wR</i> ₂ = 0.2952
Final <i>R</i> indexes [all data]	<i>R</i> ₁ = 0.0982, <i>wR</i> ₂ = 0.2096	<i>R</i> ₁ = 0.1303, <i>wR</i> ₂ = 0.3278
Largest diff. peak/hole/e Å ⁻³	0.32/-0.29	1.42/-0.63
CCDC number	1891026	1891027

except some minor differences in the corresponding bond lengths and angles. The angles between the planes of the anthracene and benzene rings of the two molecules

present in the asymmetric unit are 76.42° and 79.80°. The supramolecular analysis of **3d** revealed that the crystal structure is stabilized by a number of C–H... π

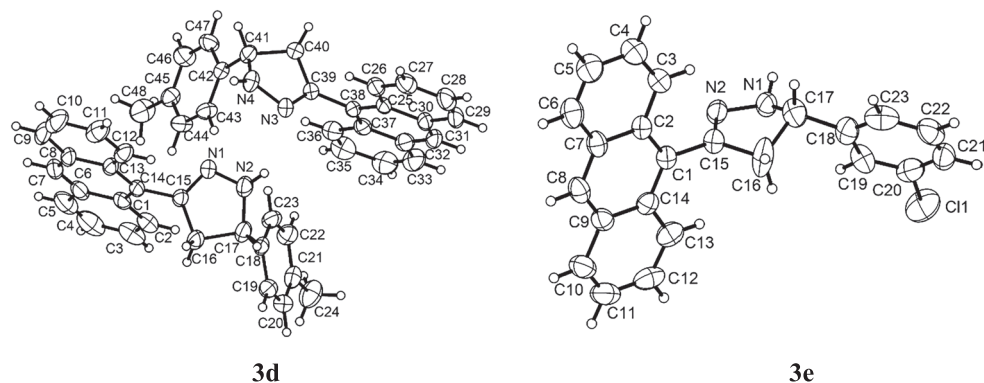


Figure 2. X-ray crystal structure thermal ellipsoid plot (30% probability level) of anthracenyl pyrazolines **3d** and **3e**.

intermolecular interactions. The strongest interaction among them is C47–H47...Cg1 with an angle of 161.62° and an H...Cg1 distance of 2.718 Å. The other such bonds include C9–H9...Cg1 with an angle of 162.06° and an H...Cg1 distance of 2.798 Å, C46–H46...Cg2 with an angle of 122.17° and an H...Cg2 distance of 3.161 Å, and C19–H19...Cg3 with an angle of 171.87° and an H...Cg3 distance of 2.757 Å; see Table S.3.1 (Cg1 is the ring centroid of the six-membered C25–38 ring, Cg2 of C25–C30, and Cg3 of C1–C14; see Fig. 2 also). The amine-H atom in **3d** does not participate in hydrogen bonding interactions. The inter-connection of molecules through such weak bonding interactions leads to a supramolecular sheet-like structure in the crystal lattice (Fig. S.3.1).

Meanwhile, compound **3e** crystallized in orthorhombic Pccn space group. The asymmetric unit consists of one molecule of **3e** as shown in Figure 2. The planes of the anthracene and phenyl rings in this molecule make an angle of 49° with each other. Structural analyses revealed a number of weak bonding interactions in the crystal.

These include various C–H...Cl, N–H...N, and C–H... π interactions (Table S.3.2). All these interactions stabilize the crystal structure and lead to the formation of a supramolecular arrangement as shown in Figure S.3.2. Crystallographic data for the solved structures **3d** and **3e** were deposited to the Cambridge Crystallographic Data Center as supplementary publication numbers CCDC-1891026 and CCDC-1891027, respectively. These data can be obtained free of charge from the Cambridge Crystallographic Data Center *via* www.ccdc.cam.ac.uk.

Biology. Anticancer activity. The anticancer activity of the newly synthesized anthracenyl pyrazoline derivatives (**3a–o**) was carried out against four human cancer cell lines MCF-7 (breast cancer), SK-N-SH (neuroblastoma cancer), HeLa (cervical cancer), and HepG2 (liver cancer). Curcumin was used as a reference drug, and the cell viability in the presence of test compounds was measured by MTT (3-(4,5-dimethylthiazolyl-2)-2,5-diphenyltetrazolium bromide) assay. The anticancer

Table 3

Anticancer inhibition values (IC₅₀) of anthracenyl pyrazoline compounds (**3a–o**) on four human cell lines.

S. no.	Compounds	Anticancer activity (IC ₅₀ ; μ M)			
		MCF-7	SK-N-SH	HeLa	HepG2
1	3a	0.73	260.00	0.22	3.86
2	3b	0.495	290.00	25.00	22.22
3	3c	3.08	254.22	29.56	3.50
4	3d	0.493	258.42	2.03	26.44
5	3e	0.66	254.23	2.58	20.88
6	3f	1.5	250.66	27.29	20.65
7	3g	1.5	240.26	1.96	19.22
8	3h	2.0	250.29	1.10	33.44
9	3i	26.0	3.55	1.30	0.22
10	3j	17.0	260.22	0.3	1.58
11	3k	1.98	1.88	1.88	0.44
12	3l	23.0	2.00	0.3	0.40
13	3m	29.0	23.42	0.10	0.22
14	3n	25.0	25.33	0.25	2.66
15	3o	2.50	253.88	0.25	3.26
16	Curcumin	50	58.33	35.00	15.23

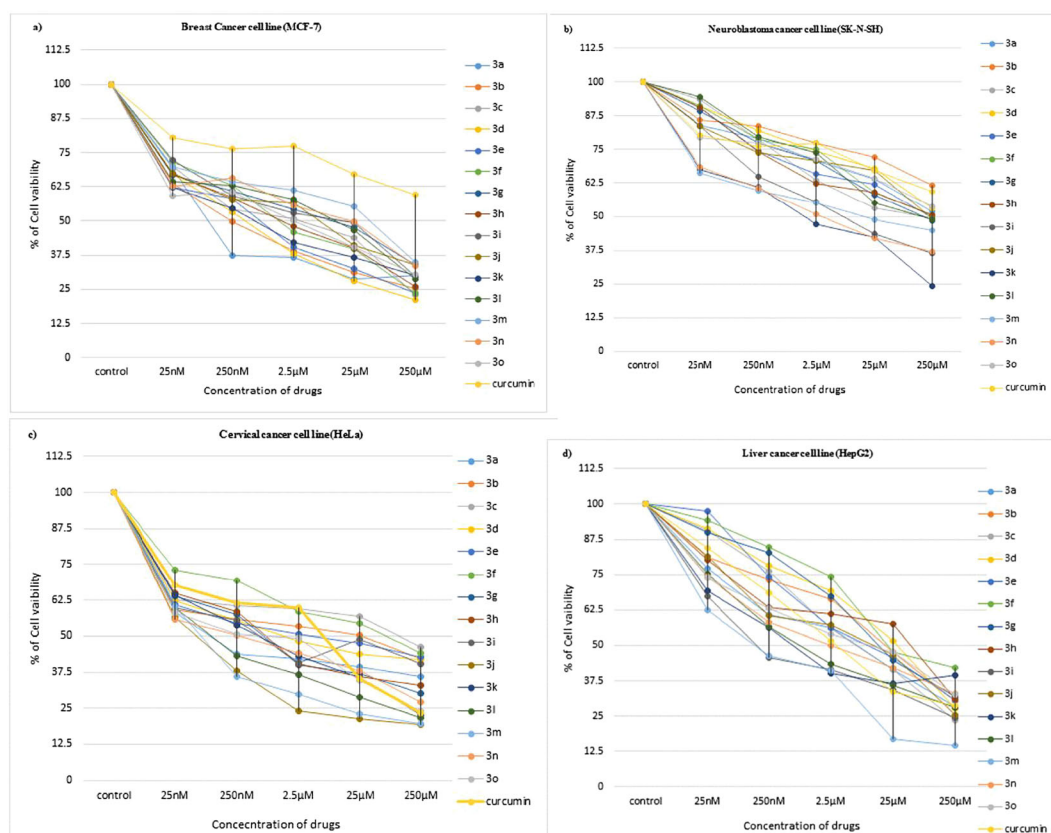


Figure 3. The survival curves of the human cancer cells (MCF-7 (a), SK-N-SH (b), HeLa (c), and HepG2 (d)) for anthracenyl pyrazoline compounds (**3a–o**); curcumin was used as a positive control. [Color figure can be viewed at wileyonlinelibrary.com]

activity results revealed that compounds **3a**, **3b**, **3d**, and **3e** exhibit a potential toxicity against MCF-7 cells (IC_{50} : 0.73, 0.495, 0.493, and 0.66 μM) and **3i**, **3k**, and **3l** showed a good toxicity against SK-N-SH cells (IC_{50} : 3.55, 1.88, and 2.00 μM), whereas compounds **3a**, **3j**, **3l**, **3m**, **3n**, and **3o** showed a highly potential toxicity against HeLa cells (IC_{50} : 0.22, 0.3, 0.3, 0.10, 0.25, and 0.25 μM) and **3i**, **3k**, **3l**, and **3m** showed a significant toxicity against HepG2 cells (IC_{50} : 0.22, 0.44, 0.40, and 0.22 μM) (Table 3).

The overall anticancer activity screening results of the anthracenyl pyrazoline compounds (**3a–o**) against four human cancer cell lines demonstrate that the substitution on phenyl ring showed marked effect on cytotoxic activity. Index of nitrogen-containing groups and electron-donating and electron-withdrawing groups on phenyl ring led to enhanced anticancer activity apart from SK-N-SH cell lines. The replacement of phenyl ring with heterocyclic ring also shows good anticancer activity against the MCF-7, HeLa, and HepG2 except for SK-N-SH cell lines. The anticancer activity screening results (IC_{50} ; μM) of compounds (**3a–o**) were represented in Table 3, and percentage of cancer cells viability of four cell lines were depicted in Figure 3.

A comparative analysis of results of the anticancer activity shows a distinct properties of the target in three cell lines with a common requirement of hydrophobic methyl for interaction; thus, active site of target in MCF-7 cells may have lower hydrophobic packet volume; thus, $-CH_3$ and $-Cl$ could exhibit significant activity compared with higher volume ($-O-CH_3$) of the side chain. In contrast, interacting target in HeLa cells possess larger space facilitating interaction with two extended side chains ($-O-CH_3$) is symmetrically, while target in HepG2 cell line is asymmetrically located to interact with two $-O-CH_3$ groups. In addition, polar oxygen may be providing additional interactions in HeLa and HepG2, while such interaction may be absent in MCF-7.

CONCLUSIONS

We have established and reported the Et_3N -prompted efficient synthesis of anthracenyl pyrazoline derivatives (**3a–o**) and their anticancer activity. The present synthetic protocol is quite simple, and obtained yields are good to excellent as pure solids by simple filtration methods. The single-crystal X-ray crystallographic structures show

intermolecular C–H... π interactions lead to the formation of supramolecular sheet-like arrangement in **3d** and C–H...Cl, N–H...N, and C–H... π interactions in **3e**. The anticancer activity screening results revealed that compounds **3a**, **3b**, **3d**, and **3e** exhibit potential toxicity against MCF-7 cells and **3i**, **3k**, and **3l** show significant toxicity against SK-N-SH cells, whereas compounds **3a**, **3j**, **3l**, **3m**, **3n**, and **3o** showed remarkable potential toxicity against HeLa cells (IC₅₀: 0.22, 0.3, 0.3, 0.10, 0.25, and 0.25 μ M) and **3i**, **3k**, **3l**, and **3m** showed highest toxicity against HepG2 cells. In conclusion, the newly synthesized anthracenyl pyrazoline derivatives were found to be a more potent activity against cancer and some of them are exclusively potent against breast cancer and cervical cancer and have more scope to explore for further investigations towards the clinical trials.

EXPERIMENTAL

Chemistry, materials, and methods. All the reagents and solvents were purchased from commercially available sources and used without further purification. Melting points were recorded in open capillaries using IKON melting point apparatus and are uncorrected. Fourier transform infrared spectra of the compounds were recorded on Perkin-Elmer spectrophotometer (Spectrum-Two) using KBr disk, and values are expressed in cm^{-1} . ¹H-NMR and ¹³C-NMR spectra for the compounds were recorded using Bruker 300 MHz spectrometer in CDCl₃ as a solvent and tetramethylsilane as an internal standard; values are given in parts per million (ppm). Mass spectra for the compounds were recorded on PE Sciex API 2000 system. Microanalytical (CHN) data were obtained with a FLASH EA 1112 Series CHNS analyzer. Progress of the reactions was monitored by TLC with silica gel plates (Merck) using ethyl acetate and *n*-hexane (3:7) as a solvent system and visualized under UV-light/iodine vapors.

General procedure for the synthesis of anthracenyl pyrazoline (3a). To a stirred solution of corresponding anthracenyl chalcone (**1a**) (0.220 g, 1 mmol), hydrazine hydrate (**2**) (0.500 g, 10 mmol) was added Et₃N (10 mol %) in ethanol (5 mL). The reaction mixture was refluxed for 24 h with continuous stirring. After completion of the reaction monitored by TLC, the solvent was removed and added ice-cold water. The pure solid product anthracenyl pyrazoline (**3a**) was collected by filtration, washed with water (three to four times) and finally with 50% ethanol, and dried. The same synthetic protocol was followed for the synthesis of all other anthracenyl pyrazoline derivatives (**3a–o**) (Scheme 1 and Fig. 1).

X-ray crystallography. Single-crystal X-ray diffraction data of **3d** and **3e** were collected on an Agilent Super

Nova diffractometer and equipped with multilayer optics, monochromatic dual source (Cu and Mo), and Eos CCD detector, using Mo-K α (0.71073 Å) radiation at 293 K. Data acquisition, reduction, and absorption correction were performed by using CrysAlisPRO program.[17] The structure was solved with ShelXS and refined on F^2 by full-matrix least-squares techniques using ShelXL program provided in Olex² (v.1.2) program package. [18,19] Anisotropic displacement parameters were applied for all the atoms, except hydrogen atoms. H atoms were calculated into their positions or located from the electron density map and refined as riding atoms using isotropic displacement parameters. The data collected for **3e** were of poor quality, despite multiple attempts of data collection. It exhibited relatively high R_1 and wR_2 values. The ratio of maximum/minimum residual density was 2.24 in this case.

Biology and anticancer activity. Cytotoxicity of compounds in cancer cell lines. Cytotoxicity assay was performed with MTT in four human cancer cell lines (MCF-7, SK-N-SH, HeLa, and HepG2 cells). Briefly, cancer cell lines were grown in Dulbecco's modified Eagle media with 10% fetal bovine serum; approximately 0.02×10^6 cells were seeded in 100 μ L of complete media. After overnight incubation, cell viability was determined by MTT reagent (5 mg/mL) assay. Test compounds (**3a–o**) at different concentrations (25 and 250 nM and 2.5, 25, and 250 μ M) were added and incubated for a period of 48 h in cell culture incubator at 37°C. At the end of the treatment, the medium was removed, and the cells were washed with 1 \times phosphate-buffered saline, and 20 μ L of MTT was added to each well and incubated for 4 h in cell culture incubator. Finally, 200 μ L of dimethyl sulfoxide was added to all the wells, and plate was gently swirled and kept in dark for 2 h at room temperature. Absorbance was measured at 570 nm in a microtiter plate reader and compared with that of the wells in which the drug is omitted (control). Curcumin was used as a positive control. Each assay was repeated at least three times and in triplicates. The IC₅₀ (concentration of 50% inhibition) value was calculated using Microsoft Excel sheet. All compounds were showed potential anticancer activity (Fig. 3).

Spectral characterization data. 3-Anthracen-9-yl-5-phenyl-4,5-dihydro-1H-pyrazole (3a). Yellow solid. Yield: 96%. mp 94–97°C. IR (KBr) cm^{-1} 3052.66 (Aromatic C–H), 3336.68 (NH) and 1590.63 (C=N). ¹H-NMR (300 MHz, CDCl₃) δ (ppm): 8.47 (s, 1H, Ar–H), 8.03–8.01 (t, Hz, 4H, Ar–H), 7.60–7.57 (d, $J = 7.38$ Hz, 2H, Ar–H), 7.48–7.45 (m, 6H, Ar–H), 7.39–7.36 (d, $J = 7.25$ Hz, 1H, Ar–H), 6.41 (s, 1H, –NH), 5.29–5.23 (t, 1H, –CH), 3.62–3.53 (dd, 1H, –CH₂), 3.23–3.14 (dd, 1H, –CH₂). ¹³C-NMR (300 MHz, CDCl₃) δ (ppm): 151.54, 142.22, 134.14, 131.43, 130.24, 128.99, 128.76, 128.05,

127.88, 127.67, 127.25, 126.54, 126.31, 125.38, 64.87, 47.62. MS (*m/z*): 323.2 (M+1). Elemental Anal. Calcd for C₂₃H₁₈N₂: C, 77.41; H, 4.80; N, 7.85. Found: C, 77.32; H, 4.85; N, 7.79.

3-Anthracen-9-yl-5-(4-chloro-phenyl)-4,5-dihydro-1H-pyrazole (3b). Yellow solid. Yield: 95%. mp 50–53°C. IR (KBr) cm⁻¹ 3052 (Aromatic C–H), 3343.44 (NH) and 1591.30 (C=N). ¹H-NMR (300 MHz, CDCl₃) δ (ppm): 8.48 (s, 1H, Ar–H), 8.01–8.00 (d, *J* = 3.46 Hz, 4H, Ar–H), 7.53–7.40 (m, 8H, Ar–H), 6.37 (s, 1H, –NH), 5.26–5.19 (t, 1H, –CH), 3.60–3.51 (dd, 1H, –CH₂), 3.16–3.07 (dd, 1H, –CH₂). ¹³C-NMR (300 MHz, CDCl₃) δ (ppm): 151.56, 140.63, 133.54, 131.41, 130.18, 129.07, 128.82, 128.16, 128.01, 127.37, 126.41, 125.42, 125.22, 64.31, 47.65. MS (*m/z*): 357.0 (M+1). Elemental Anal. Calcd for C₂₃H₁₇N₂Cl: C, 85.68; H, 5.63; N, 8.69. Found: C, 85.52; H, 5.68; N, 8.61.

3-Anthracen-9-yl-5-(4-fluoro-phenyl)-4,5-dihydro-1H-pyrazole (3c). Yellow solid. Yield: 94%. mp 76–79°C. IR (KBr) cm⁻¹ 3053.99 (Aromatic C–H), 3342.95 (NH) and 1600.83 (C=N). ¹H-NMR (300 MHz, CDCl₃) δ: 8.48 (s, 1H, Ar–H), 8.02–8.00 (t, Hz, 4H, Ar–H), 7.57–7.46 (m, 6H, Ar–H), 7.16–7.10 (t, 2H, Ar–H), 5.27–5.21 (t, 1H, –CH), 3.59–3.50 (dd, 1H, –CH₂), 3.17–3.08 (dd, 1H, –CH₂) ppm. ¹³C-NMR (300 MHz, CDCl₃) δ: 151.69, 137.83, 134.23, 131.46, 128.85, 128.33, 128.22, 128.18, 126.42, 125.46, 125.28, 116.00, 115.71, 64.37, 47.77 ppm. MS (*m/z*): 341.1 (M+1). Elemental Anal. Calcd for C₂₃H₁₇N₂F: C, 81.16; H, 5.03; N, 8.23. Found: C, 81.26; H, 5.09; N, 8.27.

3-Anthracen-9-yl-5-*p*-tolyl-4,5-dihydro-1H-pyrazole (3d).

Yellow color single crystals were obtained from methanol solution on slow evaporation at room temperature. Yield: 96%. mp 123–125°C. IR (KBr) cm⁻¹ 30544.09 (Aromatic C–H), 3326.74 (NH), and 1589.75 (C=N). ¹H-NMR (300 MHz, CDCl₃) δ: 8.47 (s, 1H, Ar–H), 8.03–8.02 (d, *J* = 2.03 Hz, 4H, Ar–H), 7.48–7.46 (t, 6H, Ar–H), 7.27–7.25 (d, *J* = 6.92 Hz, 2H, Ar–H), 6.34 (s, 1H, –NH), 5.25–5.19 (t, 1H, –CH), 3.59–3.50 (dd, 1H, –CH₂), 3.20–3.12 (dd, 1H, –CH₂), 2.40 (s, 3H, Ar–CH₃) ppm. ¹³C-NMR (300 MHz, CDCl₃) δ: 151.58, 139.29, 137.65, 131.49, 130.30, 129.69, 128.79, 128.03, 127.86, 126.53, 126.31, 125.47, 125.41, 64.78, 47.68, 21.27 ppm. MS (*m/z*): 337.1 (M+1). Elemental Anal. Calcd for C₂₄H₂₀N₂: C, 85.68; H, 5.99; N, 8.33. Found: C, 85.56; H, 5.91; N, 8.27.

3-Anthracen-9-yl-5-(3-chloro-phenyl)-4,5-dihydro-1H-pyrazole (3e). Brown color single crystals were obtained from recrystallization in acetonitrile solution on slow evaporation at room temperature. Yield: 90%. mp 104–106°C. IR (KBr) cm⁻¹ 3053.07 (Aromatic C–H), 3343.93 (NH), and 1587.78 (C=N). ¹H-NMR (300 MHz, CDCl₃) δ: 8.48–8.45 (d, *J* = 8.69 Hz, 1H, Ar–H), 8.28–8.25 (d, *J* = 8.59 Hz, 1H, Ar–H), 8.02–7.97 (m, 4H, Ar–H), 7.74–7.72 (d, *J* = 8.46 Hz, 1H, Ar–H), 7.50–7.33 (m,

5H, Ar–H), 6.76–6.73 (d, *J* = 8.16 Hz, 1H, Ar–H), 6.56–6.48 (t, 1H, –NH), 5.35–5.10 (tt, 1H, –CH), 3.73–3.44 (m, 1H, –CH₂), 3.18–3.04 (m, 1H, –CH₂). ¹³C-NMR (300 MHz, CDCl₃) δ: 151.34, 149.48, 131.34, 130.08, 128.85, 128.70, 128.29, 127.53, 127.45, 126.50, 126.25, 125.45, 125.00, 124.01, 115.45, 64.16, 47.60. MS (*m/z*): 356.9 (M⁺). Elemental Anal. Calcd for C₂₃H₁₇N₂Cl: C, 77.41; H, 4.80; N, 7.85. Found: C, 77.32; H, 4.86; N, 7.81.

3-Anthracen-9-yl-5-(4-nitro-phenyl)-4,5-dihydro-1H-pyrazole (3f). Yellow solid. Yield: 97%. mp 67–70°C. IR (KBr) cm⁻¹ 3053.73 (Aromatic C–H), 3324.08 (NH), and 1591.85 (C=N). ¹H-NMR (300 MHz, CDCl₃) δ: 8.47 (s, 1H, Ar–H), 8.02–7.99 (t, 4H, Ar–H), 7.60 (s, 1H, Ar–H), 7.49–7.31 (m, 7H, Ar–H), 6.37 (s, 1H, –NH), 5.25–5.18 (t, 1H, –CH), 3.60–3.51 (dd, 1H, –CH₂), 3.16–3.07 (dd, 1H, –CH₂). ¹³C-NMR (300 MHz, CDCl₃) δ: 151.51, 144.32, 134.86, 131.42, 130.27, 128.82, 128.17, 128.02, 126.87, 126.43, 125.44, 125.26, 124.81, 64.45, 47.61. MS (*m/z*): 367.1 (M⁺). Elemental Anal. Calcd for C₂₃H₁₇N₃O₂: C, 75.19; H, 4.66; N, 11.44. Found: C, 75.24; H, 4.71; N, 11.32.

3-Anthracen-9-yl-5-(4-bromo-phenyl)-4,5-dihydro-1H-pyrazole (3g). Yellow solid. Yield: 94%. mp 57–59°C. IR (KBr) cm⁻¹ 3052.47 (Aromatic C–H), 3343.23 (NH), and 1589.42 (C=N). ¹H-NMR (300 MHz, CDCl₃) δ: 8.47 (s, 1H, Ar–H), 8.00–7.99 (d, *J* = 3.16 Hz, 4H, Ar–H), 7.57–7.43 (m, 8H, Ar–H), 6.37 (s, 1H, –NH), 5.23–5.16 (t, 1H, –CH), 3.58–3.49 (dd, 1H, –CH₂), 3.14–3.05 (dd, 1H, –CH₂). ¹³C-NMR (300 MHz, CDCl₃) δ: 151.56, 141.13, 132.00, 131.38, 130.14, 128.81, 128.34, 128.16, 127.27, 126.40, 125.40, 125.18, 121.60, 64.31, 47.59. MS (*m/z*): 402.0 (M+1). Elemental Anal. Calcd for C₂₃H₁₇N₂Br: C, 68.84; H, 4.27; N, 6.98. Found: C, 68.75; H, 4.31; N, 6.92.

3-Anthracen-9-yl-5-(3-fluoro-phenyl)-4,5-dihydro-1H-pyrazole (3h). Brown solid. Yield: 93%. mp 86–89°C. IR (KBr) cm⁻¹ 3055.58 (Aromatic C–H), 3328.34 (NH), and 1587.74 (C=N). ¹H-NMR (300 MHz, CDCl₃) δ: 8.47 (s, 1H, Ar–H), 8.02–7.99 (t, 4H, Ar–H), 7.48–7.02 (m, 8H, Ar–H), 6.37 (s, 1H, –NH), 5.27–5.20 (t, 1H, –CH), 3.60–3.51 (dd, 1H, –CH₂), 3.17–3.08 (dd, 1H, –CH₂). ¹³C-NMR (300 MHz, CDCl₃) δ: 151.51, 131.40, 130.57, 130.46, 130.19, 128.79, 128.13, 126.39, 125.40, 125.23, 122.24, 114.88, 114.60, 113.75, 113.46, 64.44, 47.62. MS (*m/z*): 341.1 (M+1). Elemental Anal. Calcd for C₂₃H₁₇N₂F: C, 81.16; H, 5.03; N, 8.23. Found: C, 81.23; H, 5.08; N, 8.29.

3-Anthracen-9-yl-5-(3-nitro-phenyl)-4,5-dihydro-1H-pyrazole (3i). Yellow solid. Yield: 95%. mp 73–75°C. IR (KBr) cm⁻¹ 3049.76 (Aromatic C–H), 3339.50 (NH), and 1589.69 (C=N). ¹H-NMR (300 MHz, CDCl₃) δ: 8.47 (s, 1H, Ar–H), 8.03–8.02 (d, *J* = 3.14 Hz, 4H, Ar–H), 7.48–7.45 (q, 5H, Ar–H), 7.25–7.19 (t, 2H, Ar–H), 7.25–7.19 (t, 2H, Ar–H), 6.33 (s, 1H, –NH), 5.18–5.12 (t, 1H, –CH), 3.58–3.49 (dd, 1H, –CH₂), 3.21–3.13 (dd, 1H, –CH₂). ¹³C-NMR (300 MHz, CDCl₃) δ: 151.73, 147.10,

143.62, 131.45, 130.27, 129.98, 128.77, 128.50, 128.03, 126.31, 126.15, 125.41, 116.61, 114.56, 112.89, 64.85, 47.52. MS (m/z): 367.3 (M^+). Elemental Anal. Calcd for $C_{23}H_{17}N_3O_2$: C, 75.19; H, 4.66; N, 11.44. Found: C, 75.26; H, 4.59; N, 11.51.

[4-(5-Anthracen-9-yl-3,4-dihydro-2H-pyrazol-3-yl)-phenyl]-dimethyl-amine (3j). Orange solid. Yield: 93%. mp 114–116°C. IR (KBr) cm^{-1} 3048.31 (Aromatic C–H), 3297.26 (NH), and 1588.02 (C=N). 1H -NMR (300 MHz, $CDCl_3$) δ : 8.51–8.47 (d, $J = 12.45$ Hz, 1H, Ar–H), 8.08–7.94 (m, 4H, Ar–H), 7.48–7.44 (m, 5H, Ar–H), 7.32–7.25 (t, 2H, Ar–H), 6.83–6.80 (d, $J = 8.56$, 1H, Ar–H), 6.60–6.57 (d, $J = 8.75$, 1H, Ar–H), 5.21–5.14 (t, 1H, –CH), 3.55–3.46 (dd, 1H, –CH₂), 3.22–3.13 (dd, 1H, –CH₂), 2.99 (s, 6H, Ar–N (CH₃)₂). ^{13}C -NMR (300 MHz, $CDCl_3$) δ : 151.37, 149.38, 130.76, 128.74, 128.58, 127.92, 127.43, 126.38, 125.81, 125.50, 124.42, 112.96, 111.78, 64.65, 47.54, 40.79, 40.13. MS (m/z): 366.1 ($M+1$). Elemental Anal. Calcd for $C_{25}H_{23}N_3$: C, 82.16; H, 6.34; N, 11.50. Found: C, 82.25; H, 6.38; N, 11.43.

3-Anthracen-9-yl-5-furan-2-yl-4,5-dihydro-1H-pyrazole (3k). Yellow solid. Yield: 90%. mp 56–58°C. IR (KBr) cm^{-1} 3053.20 (Aromatic C–H), 3410.42 (NH), and 1586.72 (C=N). 1H -NMR (300 MHz, $CDCl_3$) δ : 8.49–8.43 (d, $J = 17.51$ Hz, 1H, Ar–H), 8.02–8.01 (d, $J = 3.12$ Hz, 4H, Ar–H), 7.50–7.46 (m, 7H, Ar–H), 6.43–6.41 (d, $J = 4.11$ Hz, 1H, –NH), 5.25–5.19 (q, 1H, –CH), 3.77–3.70 (m, 1H, –CH₂), 3.58–3.47 (m, 1H, –CH₂). ^{13}C -NMR (300 MHz, $CDCl_3$) δ : 151.38, 142.64, 134.22, 131.10, 128.87, 128.76, 126.86, 126.37, 125.59, 125.45, 124.54, 110.55, 106.51, 57.48, 43.71. MS (m/z): 313.0 ($M+1$). Elemental Anal. Calcd for $C_{21}H_{16}N_2O$: C, 80.75; H, 5.16; N, 8.97. Found: C, 80.65; H, 5.19; N, 8.91.

3-Anthracen-9-yl-5-(3,4,5-trimethoxy-phenyl)-4,5-dihydro-1H-pyrazole (3l). Yellow solid. Yield: 95%. mp 62–64°C. IR (KBr) cm^{-1} 3053.05 (Aromatic C–H), 3333.35 (NH), and 1590.28 (C=N). 1H -NMR (300 MHz, $CDCl_3$) δ : 8.48 (s, 1H, Ar–H), 8.06–8.01 (q, 4H, Ar–H), 7.48–7.45 (q, 4H, Ar–H), 6.80 (s, 2H, Ar–H), 5.22–5.15 (t, 1H, –CH), 3.95–3.89 (t, 9H, Ar–OCH₃), 3.62–3.53 (dd, 1H, –CH₂), 3.23–3.14 (dd, 1H, –CH₂). ^{13}C -NMR (300 MHz, $CDCl_3$) δ : 153.77, 151.68, 138.29, 134.20, 131.46, 130.28, 128.86, 128.15, 127.30, 126.33, 125.43, 125.33, 103.26, 65.06, 61.03, 56.34, 47.75. MS (m/z): 413.0 ($M+1$). Elemental Anal. Calcd for $C_{26}H_{24}N_2O_3$: C, 75.71; H, 5.86; N, 6.79. Found: C, 75.62; H, 5.82; N, 6.71.

3-Anthracen-9-yl-5-(3,4-dimethoxy-phenyl)-4,5-dihydro-1H-pyrazole (3m). Yellow solid. Yield: 92%. mp 63–65°C. IR (KBr) cm^{-1} 3053.51 (Aromatic C–H), 3343.60 (NH), and 1590.43 (C=N). 1H -NMR (300 MHz, $CDCl_3$) δ : 8.53–8.42 (t, 1H, Ar–H), 8.02 (s, 3H, Ar–H), 7.88–6.80 (m, 8H, Ar–H), 5.22–5.15 (t, 1H, –CH), 3.94–3.83 (m, 6H, Ar–OCH₃), 3.59–3.50 (dd, 1H, –CH₂), 3.21–3.12 (dd, 1H, –CH₂). ^{13}C -NMR (300 MHz, $CDCl_3$) δ : 151.80,

134.96, 131.49, 130.30, 128.84, 128.58, 128.28, 128.11, 126.52, 126.35, 126.05, 125.67, 125.44, 118.78, 111.46, 109.36, 64.73, 56.12, 47.74. MS (m/z): 383.1 ($M+1$). Elemental Anal. Calcd for $C_{25}H_{22}N_2O_2$: C, 78.51; H, 5.80; N, 7.32. Found: C, 78.39; H, 5.75; N, 7.38.

3-Anthracen-9-yl-5-(4-methoxy-phenyl)-4,5-dihydro-1H-pyrazole (3n). Yellow solid. Yield: 94%. mp 103–105°C. IR (KBr) cm^{-1} 3052.61 (Aromatic C–H), 3299.86 (NH), and 1581.20 (C=N). 1H -NMR (300 MHz, $CDCl_3$) δ : 8.47 (s, 1H, Ar–H), 8.02–7.99 (d, $J = 7.35$ Hz, 4H, Ar–H), 7.51–7.45 (m, 6H, Ar–H), 6.99–6.96 (d, $J = 8.53$ Hz, 2H, Ar–H), 5.24–5.17 (t, 1H, –CH), 3.84 (s, 3H, Ar–CH₃), 3.56–3.47 (dd, 1H, –CH₂), 3.19–3.10 (dd, 1H, –CH₂). ^{13}C -NMR (300 MHz, $CDCl_3$) δ : 159.26, 151.53, 134.11, 131.40, 130.20, 128.73, 127.96, 127.82, 127.68, 126.26, 125.39, 125.35, 114.28, 64.43, 55.40, 47.57. MS (m/z): 353.1 ($M+1$). Elemental Anal. Calcd for $C_{24}H_{20}N_2O$: C, 81.79; H, 5.72; N, 7.95. Found: C, 81.66; H, 5.67; N, 7.89.

4-(5-Anthracen-9-yl-3,4-dihydro-2H-pyrazol-3-yl)-pyridine (3o). Brown solid. Yield: 90%. mp 57–60°C. IR (KBr) cm^{-1} 3053.10 (Aromatic C–H), 3412.73 (NH), and 1599.03 (C=N). 1H -NMR (300 MHz, $CDCl_3$) δ : 8.64–8.63 (d, $J = 4.34$ Hz, 2H, Ar–H), 8.48 (s, 1H, Ar–H), 8.05–7.94 (m, 3H, Ar–H), 7.80–7.79 (d, $J = 4.89$ Hz, 1H, Ar–H), 7.49–7.46 (q, 6H, Ar–H), 6.43 (s, 1H, –NH), 5.25–5.18 (t, 1H, –CH), 3.65–3.56 (dd, 1H, –CH₂), 3.15–3.06 (dd, 1H, –CH₂). ^{13}C -NMR (300 MHz, $CDCl_3$) δ : 151.36, 150.18, 134.17, 131.37, 130.13, 128.86, 128.58, 128.32, 126.51, 125.45, 125.01, 121.72, 63.64, 47.26. MS (m/z): 324.2 ($M+1$). Elemental Anal. Calcd for $C_{22}H_{17}N_3$: C, 81.71; H, 5.30; N, 12.99. Found: C, 81.65; H, 5.36; N, 12.89.

Acknowledgments. Dr. Prabhakar M. highly acknowledges the SERB-DST, Govt. India, for the financial support (grant no. SB/EMEQ-030/2014) towards his research work. Thechano M. thanks the SERB-DST for the financial support and UGC, India, for NFHE. We thank Nagaland University, University of Hyderabad, and IIT-Mandi for the instrumental facilities.

REFERENCES AND NOTES

- [1] (a) Cancer stats: cancer statistics for the UK. Available at <https://www.cancerresearchuk.org/health-professional/cancer-statistics/worldwide-cancer>; (b) Global cancer facts and figures, 2nd ed. Available at <https://www.cancer.org/content/dam/cancer-org/research/cancer-facts-and-statistics/global-cancer-facts-and-figures/global-cancer-facts-and-figures-4th-edition.pdf>
- [2] Pisani, P. *Environ Health* 2011, 10, 52.
- [3] Lam, S. W.; Jimenez, C. R.; Boven, E. *Cancer* 2014, 40, 129.
- [4] Deutsch, E.; Maggiorella, L.; Eschwege, P.; Bourhis, J.; Soria, J. C.; Abdulkarim, B. *Lancet Oncol* 2004, 5, 303.
- [5] Mathur, G.; Nain, S.; Sharma, P. K. *Acad J Cancer Res* 2015, 8. <https://doi.org/10.5829/idosi.ajcr.2015.8.1.9336>.
- [6] Nepali, K.; Sharma, S.; Sharma, M.; Bedi, P. M. S.; Dhar, K. *L. Eur J Med Chem* 2014, 77, 422.
- [7] Rebutti, M.; Michiels, C. *Biochem Pharmacol* 2013, 85, 1219.

- [8] Nussbaumer, S.; Bonnabry, P.; Veuthey, J. L.; Fleury-Souverain, S. *Talanta* 2011, 85, 2265.
- [9] Elguero, J. Pyrazoles; In *Comprehensive Heterocyclic Chemistry II: A Review of the Literature 1982–1995* Katritzky, A. P.; Rees, C. W.; Scriven, E. F. V. Eds., 1st ed.; Pergamon: Oxford, 1996, pp. 1–75.
- [10] (a) Cottineau, B.; Toto, P.; Marot, C.; Pipaud, A.; Chenault, J. *Bioorg Med Chem Lett* 2002, 12, 2105; (b) Ansari, A.; Ali, A.; Asif, M. *New J Chem* 2017, 41, 16; (c) B'Bhatt, H.; Sharma, S. *Arab J Chem* 2017, 10, S1590; (d) Hernández-Vázquez, E.; Ocampo-Montalban, H.; Cerón-Romero, L.; Cruz, M.; Gómez-Zamudio, J.; Hiriart-Valencia, G.; Villalobos-Molina, R.; Flores-Flores, A.; Estrada-Soto, S. *Eur J Pharmacol* 2017, 803, 159.
- [11] (a) Lee, K. Y.; Kim, J. M.; Kim, J. N. *Tetrahedron Lett* 2003, 44, 6737; (b) Sayed, G. H.; Azab, M. E.; Anwer, K. E.; Raouf, M. A.; Negm, N. A. *J Mol Liq* 2018, 252, 329; (c) El Shehry, M. F.; Ghorab, M. M.; Abbas, S. Y.; Fayed, E. A.; Shedid, S. A.; Ammar, Y. A. *Eur J Med Chem* 2018, 143, 1463.
- [12] (a) Jia, Z. J.; Wu, Y.; Huang, W.; Zhang, P.; Song, Y.; Woolfrey, J.; et al. *Bioorg Med Chem Lett* 2004, 14, 1229; (b) Jia, H.; Bai, F.; Liu, N.; Liang, X.; Zhan, P.; Ma, C.; Jiang, X.; Liu, X. *Eur J Med Chem* 2016, 123, 202.
- [13] (a) Dewangan, D.; Kumar, T.; Alexander, A.; Nagori, K.; Tripathi, D. K. *Curr Pharm Res* 2011, 1, 369; (b) Rao, V. K.; Tiwari, R.; Chhikara, B. S.; Shirazi, A. N.; Parang, K.; Kumar, A. *RSC Adv* 2013, 3, 15396; (c) Reddy, T. S.; Kulhari, H.; Reddy, V. G.; Bansal, V.; Kamal, A.; Shukla, R. *Eur J Med Chem* 2015, 101, 790; (d) Wang, M.; Xu, S.; Lei, H.; Wang, C.; Xiao, Z.; Jia, S.; Zhi, J.; Zheng, P.; Zhu, W. *Bioorg Med Chem* 2017, 25, 5754.
- [14] (a) Elguero, J. In *Comprehensive Heterocyclic Chemistry*, I. I.; Katritzky, A. R.; Rees, C. W.; Scriven, E. F. V. Eds.; Pergamon Press: Oxford, 1996, pp 1–75; (b) Ohtsuka, Y.; Uraguchi, D.; Yamamoto, K.; Tokuhisa, K.; Yamakawa, T. *Tetrahedron* 2012, 68, 2636; (c) Gosselin, F.; O'Shea, P. D.; Webster, R. A.; Reamer, R. A.; Tillyer, R. D.; Grabowski, E. J. J. *Synlett* 2006, 2006, 3267.
- [15] (a) Fustero, S.; Simo'n-Fuentes, A.; Sanz-Cervera, J. F. *Org Prep Proc Int* 2009, 41, 253; (b) Ji, G.; Wang, X.; Zhang, S.; Xu, Y.; Ye, Y.; Li, M. *Chem Commun* 2014, 50, 4361.
- [16] Prabhakar, M.; Thechano, M.; Shurhovolie, T.; Ruokosenuo, Z.; Nishant, J.; Aaysha, S.; Sreenivas, E. *J Chem & Pharm Res* 2017, 9, 185.
- [17] CrysAlisPro Program, version 171.37.33c; Data Collection and Processing Software for Agilent X-ray Diffractometers. Agilent Technologies: Oxford. 2012;1–49.
- [18] Sheldrick, G. M. *Acta Crystallogr* 2008, A64, 112.
- [19] Dolomanov, O. V.; Bourhis, L. J.; Gildea, R. J.; Howard, J. A. K.; Puschmann, H. J. *Appl Crystallogr* 2009, 42, 339.

SUPPORTING INFORMATION

Additional supporting information may be found online in the Supporting Information section at the end of the article.